UNLIMITED SAMPLING WITH LOCAL AVERAGES

Dorian Florescu and Ayush Bhandari

Dept. of Electrical and Electronic Engg., Imperial College London, SW72AZ, UK.
Email: d.florescu@imperial.ac.uk • a.bhandari@imperial.ac.uk

ABSTRACT

Signal saturation or clipping is a fundamental bottleneck that limits the capability of analog-to-digital converters (ADCs). The problem arises when the input signal dynamic range is larger than ADC's dynamic range. To overcome this issue, an alternative acquisition protocol called the Unlimited Sensing Framework (USF) was recently proposed. This non-linear sensing scheme incorporates signal folding (via modulo non-linearity) before sampling. Reconstruction then entails "unfolding" of the high dynamic range input. Taking an end-to-end approach to the USF, a hardware validation called US-ADC was recently presented. US-ADC experiments show that, in some scenarios, the samples can be more accurately modelled as local averages than ideal, pointwise measurements. In particular, this happens when the input signal frequency is much larger than the operational bandwidth of the US-ADC. Pushing such hardware limits using computational approaches motivates the study of modulo sampling and reconstruction via local averages. By incorporating a modulo-hysteresis model, both in theory and in hardware, we present a guaranteed recovery algorithm for input reconstruction. We also explore a practical method suited for low sampling rates. Our approach is validated via simulations and experiments on hardware, thus enabling a step closer to practice.

Index Terms— Analog-to-digital conversion (ADC), average sampling, harmonic analysis, modulo samples, sampling theory.

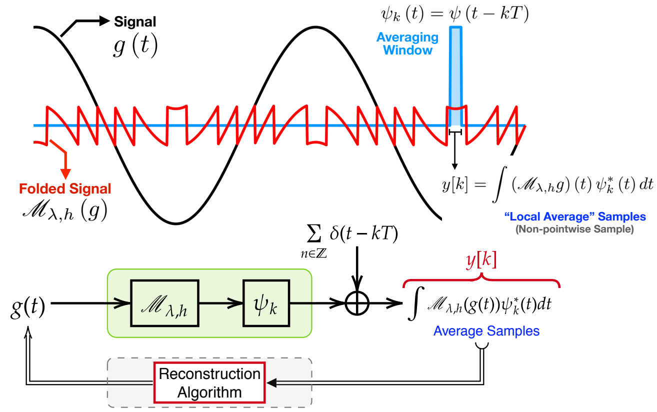

Fig. 1. Schematic and sampling pipeline of the idea of hysteresis enabled Unlimited Sampling and recovery from local averages.

1. INTRODUCTION

Practical implementation of Shannon's sampling theorem via analog-to-digital converters (ADC) suffers from a fundamental bottleneck arising from the limited dynamic range (DR) of the ADC. When signal amplitudes are larger than the ADC threshold, the resulting samples entail a permanent loss of information due to clipping and saturation. The hardware solution to this problem is to calibrate the ADC's DR to the signal of interest and this requires allocation of higher number of bits (to maintain quantization resolution). Alternatively, the computational solution is to deploy signal processing algorithms to recovery information from lossy samples.

Unlimited Sensing Approach. Realizing that *hardware-only* or *algorithms-only* solutions are inadequate, taking a fundamentally different approach to this problem, recently, the Unlimited Sensing Framework (USF) has been proposed in the literature [1–6]. The USF approach goes beyond the hardware-only or algorithms-only philosophy and instead, takes a *computational sensing* approach where the goal is to jointly harness a collaboration between hardware and algorithms. To this end, a modulo non-linearity is implemented in the hardware so that continuous-time, high dynamic range (HDR) signals are folded back into the ADC's DR. Thereafter, the inverse problem of recovering the HDR signal from folded samples is solved using mathematically guaranteed recovery algorithms. An *end-to-end* implementation of the USF based on modulo ADC and a new Fourier-Prony recovery method is presented in [5]. Recently, we introduced a new model called *modulo-hysteresis*, which enabled introducing recovery guarantees for a different class of inputs in noisy scenarios [6].

USF based acquisition not only applies to different sampling models [7, 8] but also extends to topics such as sensor array processing [9, 10] and computational imaging [11–13]. Community wide efforts include, *i)* different methods for sampling and reconstruction [14–16], *ii)* study of sparse recovery [17–19], *iii)* algorithms for signal de-noising [20–22], *iv)* development of multi-channel models [23], *v)* design of digital communication systems [24] and *vi)* more recently, design of an optical ADC [25].

Motivation. In developing the modulo sampling hardware, viz. the US-ADC [5], we have observed that in certain practical scenarios, ideal, pointwise sampling assumption[1] may not hold. Instead, as validated by our hardware experiment in Section 4, a more reasonable model entails *local average* of the sample values; conceptually, this is shown in Fig. 1. This manifestation is particularly conspicuous when the US-ADC is pushed to its limits by feeding input signals of bandwidth much higher than its operational bandwidth. This scenario frequently arises in communication systems and understand-

This research is supported by the UK Research and Innovation council's Future Leaders Fellowship program "Sensing Beyond Barriers" (MRC Fellowship award no. MR/S034897/1). Further details on Unlimited Sensing and upcoming materials on *reproducible research* are available via `https://bit.ly/USF-Link`.

[1]That is, integration with Dirac distribution or $\delta(t)$.

ably, the topic of *average sampling* traces its roots to the work of Wiley *et al*. [26] in wide-band FM communications (circa 1977). In the last many years, several authors have devoted research efforts towards approximation theoretic understanding of the *average sampling* problem, both for bandlimited classes [27, 28] and shift-invariant spaces [29]. The problem of non-uniform or irregular sampling has also been discussed [30].

Contributions. In taking the theoretical underpinnings of the USF approach all the way to practice, we believe that a thorough understanding of the *average sampling* context is quite pertinent. Furthermore, from a computational sensing perspective, we find that pushing a hardware apparatus (*e.g.* US-ADC) beyond its limits using computational methods is an attractive feature of the overall USF pipeline. Towards these goals, our key contributions are as follows: *i*) We formalize the problem of sampling and reconstruction of bandlimited functions from local averages of its modulo representation. To our knowledge, this is the first work to addresses this problem, *ii*) In the context of the *modulo-hysteresis* model, we develop mathematically guaranteed reconstruction algorithms. and *iii*) We provide a validation of our approach using both numerical simulations and hardware experiments.

2. PROBLEM FORMULATION

Here we review the new sampling pipeline, and subsequently derive input recovery guarantees. The modulo operator is given by [2],

$$\mathscr{M}_\lambda\left(g\left(t\right)\right)=2\lambda\left(\left[\!\left[\frac{g\left(t\right)}{2\lambda}+\frac{1}{2}\right]\!\right]-\frac{1}{2}\right),\qquad [\![g]\!]=g-\lfloor g\rfloor \quad (1)$$

where $\lfloor g\rfloor=\sup\left\{k\in\mathbb{Z}|\, k\leqslant g\right\}$ is the floor function. This function was generalized, by introducing an additional parameter $h\in\mathbb{R}$, to an operator $\mathscr{M}_{\mathsf{H}}:PW_\Omega\to L^2\left(\mathbb{R}\right),\mathsf{H}=[\lambda\; h]$, such that $\mathscr{M}_{\mathsf{H}}g\left(t\right)=\mathscr{M}_\lambda\left(g\left(t\right)\right)$ for $h=0$ [6], where PW_Ω is the Paley-Wiener space of Ω–bandlimited functions, and $L^2\left(\mathbb{R}\right)$ is the space of functions with finite energy. Here, h models a memory property of the sampler, called hysteresis, which means that the modulo output no longer depends only on the instantaneous input, but on the whole input history. We introduce the formal definition below.

Definition 1 (Modulo-Hysteresis)**.** *The operator $\mathscr{M}_{\mathsf{H}}$ with threshold λ and hysteresis $h\in[0,\lambda)$, where $\mathsf{H}=[\lambda\; h]$, generates a sequence $\{\tau_r\}$ and a function $z\left(t\right), t\geqslant\tau_0$ for input $g\in PW_\Omega$, such that*

$$z\left(t\right)=g\left(t\right)-\varepsilon_g\left(t\right), \quad (2)$$

where $\varepsilon_g\left(t\right)=2\lambda_h\sum_{r\in\mathbb{Z}}s_r\mathbb{1}_{[\tau_r,\infty)}\left(t\right)$, $\mathbb{1}_S$ is the indicator function, $s_r=\operatorname{sign}\left(g\left(\tau_r\right)-g\left(\tau_{r-1}\right)\right), r\geqslant 1$, $\lambda_h\triangleq\lambda-h/2$, and

$$\begin{aligned}\tau_1&=\min\left\{t>\tau_0|\mathscr{M}_\lambda\left(g\left(t\right)+\lambda\right)=0\right\},\\ \tau_{r+1}&=\min\left\{t>\tau_r|\mathscr{M}_\lambda\left(g\left(t\right)-g\left(\tau_r\right)+hs_r\right)=0\right\}.\end{aligned}$$

A key property of the modulo-hysteresis encoder is that $\tau_{r+1}-\tau_r\geqslant\min\left\{h,2\lambda_h\right\}/\left(\Omega g_\infty\right)$ [8], or any two folding times are bounded in separation. Assuming the input is bandlimited $g\in PW_\Omega$ and that the averaging kernel ψ is compactly supported $\operatorname{supp}\left(\psi\right)\in[-\nu,\nu]$. The modulo-hysteresis average samples $\{y\left[k\right]\}$ satisfy

$$y\left[k\right]=\left\langle\mathscr{M}_{\mathsf{H}}g\left(\cdot\right),\psi\left(\cdot-kT\right)\right\rangle=\mathscr{M}_{\mathsf{H}}g*\overline{\psi}\left(kT\right), \quad (3)$$

where $\langle\cdot,\cdot\rangle$ denotes the inner product, $\overline{\psi}\left(t\right)=\psi\left(-t\right)$ and $*$ is the convolution operator. For the particular case of *an ideal averaging kernel [26]*, $\psi\left(t\right)=\left(\frac{1}{2\nu}\right)\mathbb{1}_{[-\nu,\nu]}\left(t\right)$. Combining (2,3), we obtain,

$$\begin{aligned}y\left[k\right]&=\left\langle g-\varepsilon_g,\psi\left(\cdot-kT\right)\right\rangle\\&=\frac{1}{2\nu}\int_{kT-\nu}^{kT+\nu}g\left(s\right)ds-2\lambda_h\sum_{r\in\mathbb{Z}}s_r\left\langle\mathbb{1}_{[\tau_r,\infty)},\psi\left(\cdot-kT\right)\right\rangle\\&=g\left(t_k\right)-\sum_{r\in\mathbb{Z}}\tfrac{s_r\lambda_h}{\nu}\int_{\mathbb{M}}1ds,\end{aligned} \quad (4)$$

where $t_k\in[kT-\nu,kT+\nu]$, $g\left(t_k\right)$ is determined by the *mean value theorem*, and $\mathbb{M}=[kT-\nu,kT+\nu]\cap[\tau_r,\infty)$. We have that

$$\left(\frac{\lambda_h}{\nu}\right)\int_{\mathbb{M}}1ds=\begin{cases}2\lambda_h, & \tau_r\leqslant kT-\nu,\\ \frac{\lambda_h}{\nu}\left(\nu+kT-\tau_r\right), & \tau_r\in\left(kT-\nu,kT+\nu\right),\\ 0, & \tau_r\geqslant kT+\nu.\end{cases} \quad (5)$$

A direct calculation shows that

$$y\left[k\right]=g\left(t_k\right)-\varepsilon_\nu\left(kT\right),\quad \varepsilon_\nu\left(t\right)\triangleq\sum\nolimits_{r\in\mathbb{Z}}s_r\varepsilon_0\left(t-\tau_r\right) \quad (6)$$

where $\varepsilon_0\left(t\right)=\left(t+\nu\right)\frac{\lambda_h}{\nu}\mathbb{1}_{[-\nu,\nu]}\left(t\right)+2\lambda_h\cdot\mathbb{1}_{[\nu,\infty)}\left(t\right)$.

When comparing $\varepsilon_\nu\left(t\right)$ to $\varepsilon_g\left(t\right)$ (2), we note that the exact step function $\mathbb{1}_{[\tau_r,\infty)}$ from $\varepsilon_g\left(t\right)$ is replaced by a step function $\varepsilon_0\left(t\right)$ with the same amplitude $2\lambda_h$, but with a *transient period* of duration 2ν and slope λ_h/ν. The transient period is a direct consequence of average sampling, and can be designed by choosing an appropriate averaging kernel ψ. The short transient periods present in the residual function at the folding times were implicitly modelled in a phenomenological sense in [6] to explain non-ideal folding in hardware measurements. However, in the present case of average sampling, the measurements are described by different sampling paradigms on each of the two modulo signal components: non-uniform sampling of $g\left(t\right)$ and uniform sampling of $\varepsilon_\nu\left(t\right)$ (6). To recover g, one needs to eliminate $\varepsilon_\nu\left(kT\right)$ in (6). We define the finite difference operator Δ^N for a sequence $\{a_k\}$ recursively as $\Delta^N a_k=\Delta^{N-1}a_{k+1}-\Delta^{N-1}a_k$ such that $\Delta^0 a_k=a_k$. Then

$$\Delta^N y\left[k\right]=\Delta^N g\left(t_k\right)-\Delta^N e\left[k\right],\quad e\left[k\right]\triangleq\varepsilon_\nu\left(kT\right). \quad (7)$$

In USF, the input is recovered by annihilating $\varepsilon_g\left(kT\right)$ from $\Delta^N y\left[k\right]$, by leveraging the fact that $\varepsilon_g\left(kT\right)\in 2\lambda\cdot\mathbb{Z}$. This is possible because Δ^N shrinks $g\left(kT\right)$ but always leaves $\varepsilon_g\left(kT\right)$ on an equally spaced grid that is then annihilated via a modulo operation. This is no longer true for average sampling, where $\varepsilon_\nu\left(kT\right)=e\left[k\right]\in\mathbb{R}$. However, as will be shown next, $g\left(t_k\right)$ are highly correlated for a high enough sampling rate. Conversely, $\varepsilon_\nu\left(t\right)$ is not bandlimited, and thus $e\left[k\right]$ are not well correlated. As N increases, we show that Δ^N vanishes gradually $g\left(t_k\right)$, while increasing indefinitely $e\left[k\right]$.

To quantify $\Delta^N g\left(t_k\right)$, we interpret the sampling times $\{t_k\}$ as uniform instants $\{kT\}$ jittered by bounded noise. We reformulate the timing jitter as amplitude errors, $\eta\left[k\right]\triangleq g\left(t_k\right)-g\left(kT\right)$. Thus,

$$\left|\eta\left[k\right]\right|=\left|g\left(t_k\right)-g\left(kT\right)\right|\leqslant\|g'\|_\infty\cdot\left|kT-t_k\right|=\|g'\|_\infty\nu. \quad (8)$$

Then we have $\left|\Delta^N g\left(t_k\right)\right|\leqslant\left|\Delta^N g\left(kT\right)\right|+\left|\Delta^N\eta\left[k\right]\right|$ where $\left|\Delta^N g\left(kT\right)\right|\leqslant\left(T\Omega e\right)^N\|g\|_\infty$ was proved in [2] and the second term is bounded using (8), $\left|\Delta^N\eta\left[k\right]\right|\leqslant\nu 2^N\Omega\|g\|_\infty$ and hence,

$$\left|\Delta^N g\left(t_k\right)\right|\leqslant\left(T\Omega e\right)^N\|g\|_\infty+\nu 2^N\Omega\|g\|_\infty. \quad (9)$$

Algorithm 1: Average Sampling Recovery Algorithm.

Data: $y[k], N, \lambda, h, \nu, \Omega > 0$.
Result: $\widetilde{g}(t)$.

1) Compute $\Delta^N y[k]$.
2) Compute R, $\{k_m^r\}_{r=1}^R$ with (14) and (15).
3) For $r = 1, \ldots, R$
   4.1) Compute $\widetilde{n}_r = k_m^r + N$.
   4.2) If $\left|\Delta^N y[k_m^r]\right| > 2\lambda_h - \frac{\lambda_h}{2N}$, compute $\widetilde{\beta}_r = 1$.
   4.3) If $\left|\Delta^N y[k_m^r]\right| \leqslant 2\lambda_h - \frac{\lambda_h}{2N}$, compute $\widetilde{\beta}_r = \frac{\left|\Delta^N y[k_m^r]\right|}{2\lambda_h}$.
   4.4) Compute $\widetilde{\tau}_r = \widetilde{n}_r T - 2\nu\widetilde{\beta}_r + \nu$.
   4.5) Compute $s_r = -\text{sign}\left(\Delta^N y[k_m^r]\right)$.
4) Compute $\widetilde{\varepsilon}_\nu(kT)$ using (17)
5) Compute $\widetilde{\mathbf{c}}$ using $\widetilde{\mathbf{c}} = \mathbf{M}^+\mathbf{g}$.
6) Compute $\widetilde{g}(t) = \sum_{k\in\mathbb{Z}} [\widetilde{\mathbf{c}}]_k \operatorname{sinc}_\Omega(t - kT)$.

Recovery with a Single Fold. For simplicity, we first assume a single folding time $\tau_1 > 0$. From Lemma 2 in [6], we have $\Delta^N e[k]$ are non-zero close to the indices of the folding samples n_r. Specifically, it can be shown that $\text{supp}\left(\Delta^N e\right) \subseteq \{n_r - N, \ldots, n_r\}$. To estimate $e[k]$ from $y[k]$ we assume a smoothness property on $g(t_k)$, *i.e.* $\|\Delta^N g(t_k)\|_\infty < \frac{\lambda_h}{2N}$. We note that far away from the jump, this condition will also hold for $y[k]$ in place of $g(t_k)$. This implies,

$$\mathbb{M}_N \triangleq \left\{k \in \mathbb{Z} \mid \left|\Delta^N y[k]\right| \geqslant \frac{\lambda_h}{2N}\right\} \tag{10}$$

is in the vicinity of the jump and can be used to estimate the jump location up to a minimal ambiguity. Specifically, the jump τ_1 is determined by computing $k_m = \min \mathbb{M}_N$ via thresholding, as shown in the following theorem (the proof follows closely Theorem 1 in [6]).

Theorem 1 (Estimation of Folding Times). *Assume* $\|\Delta^N g(t_k)\|_\infty < \lambda_h/2N$ *and let* $k_m = \min \mathbb{M}_N$ (10). *Furthermore, let* $\widetilde{\tau}_1 = \widetilde{n}_1 T - 2\nu\widetilde{\beta}_1 + \nu$ *and* $\widetilde{s}_1 = -\text{sign}\left(\Delta^N y[k_m]\right)$ *be the estimates of the folding time with* $\widetilde{n}_1 = k_m + N$ *and* $\widetilde{\beta}_1$ *given by*

$$\begin{cases} \left|\Delta^N y[k_m]\right| \leqslant 2\lambda_h - \frac{\lambda_h}{2N} & \text{then } \widetilde{\beta}_1 \to \frac{\Delta^N y[k_m]}{2\lambda_h \widetilde{s}_1}, \\ \left|\Delta^N y[k_m]\right| > 2\lambda_h - \frac{\lambda_h}{2N} & \text{then } \widetilde{\beta}_1 \to 1. \end{cases}$$

Then $\widetilde{s}_1 = s_1$, $\widetilde{n}_1 \in \{n_1, n_1+1\}$, *and the following holds*

$$k_m = \begin{cases} n_1 - N & \widetilde{n}_1 = n_1, |\widetilde{\tau}_1 - \tau_1| \leqslant \frac{\nu}{2N} \\ n_1 - N + 1 & \widetilde{n}_1 = n_1 + 1, |\widetilde{\tau}_1 - \tau_1| \leqslant T + \nu\left(\frac{3}{4N} - \frac{1}{2}\right) \end{cases}$$

Theorem 1 shows that for small enough averaging window size ν and high enough N, the folding times can be recovered with high precision. In fact, for $N \geqslant 2$, the result recovers τ_1 with an error strictly smaller than T, which is the smallest error that can be guaranteed with USF. The input average samples are computed with

$$\widetilde{g}(t_k) = y[k] + s_1\varepsilon_0(kT - \widetilde{\tau}_1), \tag{11}$$

where $\widetilde{g}(t_k) = g(t_k) + 2n\lambda_h, n \in \mathbb{Z}$.

Recovery with Multiple Folds. Assuming R folding times $\{\tau_r\}_{r=1}^R$, $\widetilde{g}(t_k)$ can be computed from $\widetilde{\tau}_r$ and $\widetilde{s}_r$ with Theorem 1 sequentially, if the supports of any two distinct filtered folds τ_{r_1}, τ_{r_2} are disjoint, i.e., $\{n_{r_1} - N, \ldots, n_{r_1}\} \cap \{n_{r_2} - N, \ldots, n_{r_2}\} = \emptyset$. In other words, this requires the separation of the folding samples $n_{r+1} - n_r \geqslant N + 1$ [8]. The recovery guarantees are presented in the following lemma.

Algorithm 2: Low Sampling Rate Recovery Algorithm.

Data: $y[k], N, \lambda, h, \nu, \Omega > 0$.
Result: $\widetilde{g}(t)$.

1) Compute $y_{1,N}[k] = \Delta^N y[k]$.
2) For $r = 1, \ldots, R$
   4.1) Compute $k_m^r = \min\left\{k \mid |y_{r,N}[k]| \geqslant \frac{\lambda_h}{2N}\right\}$.
   4.2) Compute $\widetilde{n}_r = k_m^r + N$.
   4.3) If $|y_{r,N}[k_m^r]| > 2\lambda_h - \frac{\lambda_h}{2N}$, compute $\widetilde{\beta}_r = 1$.
   4.4) If $|y_{r,N}[k_m^r]| \leqslant 2\lambda_h - \frac{\lambda_h}{2N}$, compute $\widetilde{\beta}_r = \frac{|y_{r,N}[k_m^r]|}{2\lambda_h}$.
   4.5) Compute $\widetilde{\tau}_r = \widetilde{n}_r T - 2\nu\widetilde{\beta}_r + \nu$.
   4.6) Compute $s_r = -\text{sign}\left(\Delta^N y[k_m^r]\right)$.
   4.7) Compute $e_{r,N}[k]$ using (18).
   4.8) If $r < R$, compute $y_{r+1,N}[k] = y_{r,N}[k] + e_{r,N}[k]$.
3) Compute $\widetilde{\varepsilon}_\nu(kT)$ using (17)
4) Compute $\widetilde{\mathbf{c}}$ using $\widetilde{\mathbf{c}} = \mathbf{M}^+\mathbf{g}$.
5) Compute $\widetilde{g}(t) = \sum_{k\in\mathbb{Z}} [\widetilde{\mathbf{c}}]_k \operatorname{sinc}_\Omega(t - kT)$.

Lemma 1 (Sufficient Recovery Conditions). *The folding times* τ_r *and signs* s_r *can be recovered from average sampling measurements* $y[k]$ *if* $\nu \leqslant T/2$ *and the following hold*

$$(T\Omega e)^N \|g\|_\infty + \nu 2^N \|g\|_\infty < \frac{\lambda_h}{2N} \tag{12}$$

$$T\Omega\|g\|_\infty (N+1) \leqslant \min\{h, 2\lambda_h\}. \tag{13}$$

In the following, we give a practical solution for computing $\{\tau_r, s_r\}$. Let $y^{[N]}[k] = \left|\Delta^N y[k]\right|$ and $\{k_m^r\}_{r=1}^R$ be the set,

$$k_m^1 = \min\left\{k \mid y^{[N]}[k] \geqslant \lambda_h/2N\right\}, \tag{14}$$

$$k_m^r = \min\left\{k > k_m^{r-1} + N \mid y^{[N]}[k] \geqslant \lambda_h/2N\right\}, \tag{15}$$

for $r = 2, \ldots, R$. By applying sequentially Theorem 1 we have

$$\widetilde{s}_r = s_r, \quad |\widetilde{\tau}_r - \tau_r| < \max\left\{\frac{\nu}{2N}, T - \nu\left(\frac{3}{4N} - \frac{1}{2}\right)\right\}. \tag{16}$$

Input Reconstruction. The input signal is recovered from $\mathcal{L}\widetilde{g}[k] = 2\nu\left(y[k] + \widetilde{\varepsilon}_\nu[kT]\right)$ (6), where $\mathcal{L}\widetilde{g}[k] \triangleq \int_{kT-\nu}^{kT+\nu} \widetilde{g}(s)\,ds$ are the local averages and

$$\widetilde{\varepsilon}_\nu(kT) = \sum_{r\in\mathbb{Z}} s_r\left(kT + \nu - \widetilde{\tau}_r\right)\frac{\lambda_h}{\nu}\mathbb{1}_{[-\nu,\nu]}(t - \widetilde{\tau}_r) \tag{17}$$

It was shown that $\widetilde{g}$ is uniquely determined by $\mathcal{L}f[k]$ if $\nu < T/2$ and $T < 1/\left(\Omega\sqrt{2}\right)$ [31]. We use the expansion $g(t) = \sum_{k\in\mathbb{Z}} c_k \operatorname{sinc}_\Omega(t - kT)$, where $\operatorname{sinc}_\Omega(t)$ is an ideal low-pass filter with bandwidth Ω. Given N samples $\{y[k]\}_{k=1}^N$, the sampled measurements can be written in matrix form as $\mathbf{Mc} = \mathbf{g}$, where $[\mathbf{M}]_{n,k} = \int_{nT-\nu}^{nT+\nu} \operatorname{sinc}_\Omega(s - kT)\,ds$, $[\mathbf{c}]_k = c_k$ and $[\mathbf{g}]_n = \mathcal{L}g[n], 1 \leqslant k, n \leqslant N$. Then we estimate $\widetilde{\mathbf{c}} = \mathbf{M}^+\mathbf{g}$ where $\mathbf{M}^+$ denotes the pseudoinverse of matrix $\mathbf{M}$. The recovery can be summarised in Algorithm 1.

3. AVERAGE SAMPLING AT LOW RATES

Here we show how the proposed algorithm can be extended to much lower sampling rates than imposed by (12,13). The most conservative of the two is (13), which enforces a minimum of N samples in

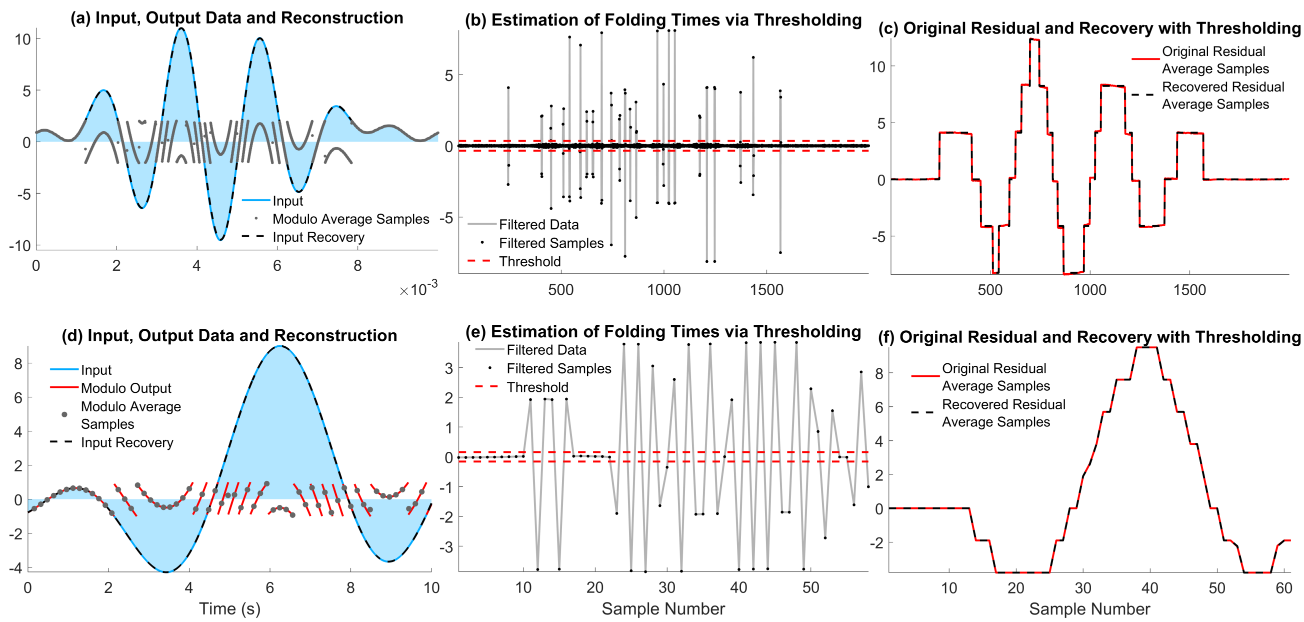

Fig. 2. Reconstruction from average samples. (a-c) Hardware experiment: Bandlimited input recovery with Algorithm 1 (a) A sum of two sin functions, continuous modulo output and 1996 acquired average samples. (b) Filtered data and fold estimation via thresholding. (c) The reconstruction of the residual function. (d-f) Recovery from modulo average sampling at low rates with Algorithm 2 from 61 samples.

between any two adjacent folds $\{\tau_r, \tau_{r+1}\}$. A small variation of the proposed recovery can still work as long as there is a region of N unfolded samples, which typically is true for much lower sampling rates. We use that $\Delta^N y[k] = \Delta^N g(t_k) - \sum_{r=1}^{R} e_{r,N}[k]$ [6], where

$$e_{r,N}[k] \triangleq b_0 \left(\widetilde{\beta}_r \Delta^{N-1}[k - \widetilde{n}_r + 1] + \left(1 - \widetilde{\beta}_r\right) \Delta^{N-1}[k - \widetilde{n}_r] \right) \tag{18}$$

where $b_0 = 2\lambda_h s_r$. We start from an anchor point sample k_0 such that $y[k] = g(t_k) + M, k \in \{k_0, \ldots, k_0 + N\}$ for some $M \in \mathbb{R}$, and identify τ_r, s_r, β_r corresponding to the folding time immediately following k_0. Then the contribution of this fold to the measurements, given by $e_{r,N}[k]$, is removed from the data via $y_{2,N}[k] = \Delta^N y[k] + e_{r,N}[k]$, and the process continues recursively (see Algorithm 2). Assuming the existence of k_0, condition (13) can be replaced by a much more relaxed condition $T\Omega \|h\|_\infty \leqslant \min\{h, \lambda_h\}$. This new condition ensures, via the hysteresis parameter h, that $\tau_r \leqslant kT \leqslant \tau_{r+1}$. As shown numerically in the next section, the existence of k_0 takes place naturally in a practical scenario.

4. NUMERICAL AND HARDWARE EXPERIMENTS

Hardware Validation. To evaluate the practical applicability of Algorithm 1, we start with a measurements based on our US-ADC [5], where the hysteresis feature was implemented in [6]. The input is an *amplitude modulated* signal generated as a sum of two sin waves, bandlimited to $3.8 \cdot 10^3$ rad/s in the DR $[-10.43, 10]$. The modulo parameters are $\lambda = 2$ and $h = 0.11$. Oversampling with $T = 5$ μsec elucidates the effect of average sampling, which determines non-ideal samples located near the modulo discontinuity Fig. 2. The width of the averaging kernel ψ was subsequently estimated form the data, as half of the average transient duration $\nu = 2.5 \cdot 10^{-6}$. The input was recovered via Algorithm 1 for $N = 3$, which resulted in error $\mathsf{Err}(g, \widetilde{g}) = 1.67\%$.

Input Recovery at Lower Sampling Rates. Algorithm 2 was then validated with a random non-periodic input computed as a sum of sinc functions bandlimited to 1.5 rad/s, centered in 5 points uniformly spaced by π/Ω in $[0, 10]$. The sinc coefficients were randomly generated using a uniform distribution on $[-20, 20]$. The modulo parameters are $\lambda = 1, h = 0.1$. The continuous modulo output $z(t)$ is subsequently sampled with averaging kernel $\psi(t) = \frac{1}{2\nu}\mathbb{1}_{[-\nu,\nu]}$ centered in uniformly spaced samples $\{kT\}_{k=1}^{249}$ where $\nu = 2 \cdot 10^{-2}$ and $T = 16 \cdot 10^{-2}$, which represents 25% of the sampling rate admitted by (13). The input, output, and average samples are depicted in Fig. 2(d). Algorithm 2 is applied for $N = 3$ to estimate the 24 folding times (Fig. 2(e)). The true and reconstructed residual, are in Fig. 2(f). The input estimation $\widetilde{g}$ is depicted in Fig. 2(d).

5. CONCLUSIONS

Motivated by the practical aspects of unlimited sampling, in particular, observations made from hardware experiments, we studied the problem of modulo sampling and recovery from local averages. By considering the modulo-hysteresis model for acquisition, we developed theoretical guarantees under which a bandlimited input can be recovered. Additionally, we investigated a practical algorithm that works at significantly lower sampling rates than what is required by the theoretical conditions. Even though traditional average sampling approaches require knowing the averaging window length, we show that the folding instants of the modulo operator enable a more convenient estimation of the window length, directly from the average samples. We validated our algorithms on synthetic and hardware data, demonstrating the practical utility of our approach.

6. REFERENCES

[1] A. Bhandari, F. Krahmer, and R. Raskar, “On unlimited sampling,” in *Intl. Conf. on Sampling Theory and Applications (SampTA)*, 2017, pp. 31–35.

[2] ——, “On unlimited sampling and reconstruction,” *IEEE Trans. Sig. Proc.*, vol. 69, pp. 3827 – 3839, Dec. 2020.

[3] ——, “Unlimited sampling of sparse signals,” in *IEEE Intl. Conf. on Acoustics, Speech and Sig. Proc. (ICASSP)*, 2018, pp. 4569–4573.

[4] A. Bhandari and F. Krahmer, “On identifiability in unlimited sampling,” in *Intl. Conf. on Sampling Theory and Applications (SampTA)*, 2019, pp. 1–4.

[5] A. Bhandari, F. Krahmer, and T. Poskitt, “Unlimited sampling from theory to practice: Fourier-Prony recovery and prototype ADC,” *IEEE Trans. Sig. Proc.*, pp. 1–1, Sep. 2021.

[6] D. Florescu, F. Krahmer, and A. Bhandari, “The surprising benefits of hysteresis in unlimited sampling: Theory, algorithms and experiments,” *IEEE Trans. Sig. Proc.*, vol. 70, pp. 616 – 630, 2022.

[7] O. Graf, A. Bhandari, and F. Krahmer, “One-bit unlimited sampling,” in *IEEE Intl. Conf. on Acoustics, Speech and Sig. Proc. (ICASSP)*, 2019, pp. 5102–5106.

[8] D. Florescu, F. Krahmer, and A. Bhandari, “Event-driven modulo sampling,” in *IEEE Intl. Conf. on Acoustics, Speech and Sig. Proc. (ICASSP)*, 2021, pp. 5435–5439.

[9] S. Fernández-Menduina, F. Krahmer, G. Leus, and A. Bhandari, “DoA estimation via unlimited sensing,” in *European Sig. Proc. Conf. (EUSIPCO)*, 2020, pp. 1866–1870.

[10] S. Fernandez-Menduina, F. Krahmer, G. Leus, and A. Bhandari, “Computational array signal processing via modulo non-linearities,” *IEEE Trans. Sig. Proc.*, 2021, doi: 10.1109/TSP.2021.3101437.

[11] A. Bhandari and F. Krahmer, “HDR imaging from quantization noise,” in *IEEE Intl. Conf. on Image Proc. (ICIP)*, 2020, pp. 101–105.

[12] A. Bhandari, M. Beckmann, and F. Krahmer, “The modulo Radon transform and its inversion,” in *European Sig. Proc. Conf. (EUSIPCO)*, 2020, pp. 770–774.

[13] M. Beckmann, F. Krahmer, and A. Bhandari, “HDR tomography via modulo Radon transform,” in *IEEE Intl. Conf. on Image Proc. (ICIP)*, 2020, pp. 3025–3029.

[14] S. Rudresh, A. Adiga, B. A. Shenoy, and C. S. Seelamantula, “Wavelet-based reconstruction for unlimited sampling,” in *IEEE Intl. Conf. on Acoustics, Speech and Sig. Proc. (ICASSP)*, 2018, pp. 4584–4588.

[15] O. Ordentlich, G. Tabak, P. K. Hanumolu, A. C. Singer, and G. W. Wornell, “A modulo-based architecture for analog-to-digital conversion,” *IEEE J. Sel. Topics Signal Process.*, vol. 12, no. 5, pp. 825–840, 2018.

[16] E. Romanov and O. Ordentlich, “Above the Nyquist rate, modulo folding does not hurt,” *IEEE Signal Process. Lett.*, vol. 26, no. 8, pp. 1167–1171, 2019.

[17] O. Musa, P. Jung, and N. Goertz, “Generalized approximate message passing for unlimited sampling of sparse signals,” in *IEEE Global Conf. on Signal and Information Proc.*, 2018, pp. 336–340.

[18] D. Prasanna, C. Sriram, and C. R. Murthy, “On the identifiability of sparse vectors from modulo compressed sensing measurements,” *IEEE Signal Process. Lett.*, vol. 28, 2020.

[19] V. Shah and C. Hegde, “Sparse signal recovery from modulo observations,” *EURASIP J. on Advances in Sig. Proc.*, vol. 2021, no. 1, 2021.

[20] M. Cucuringu and H. Tyagi, “Provably robust estimation of modulo 1 samples of a smooth function with applications to phase unwrapping,” *Journal of Machine Learning Research*, vol. 21, no. 32, 2020.

[21] M. Fanuel and H. Tyagi, “Denoising modulo samples: k-nn regression and tightness of SDP relaxation,” May 2021, preprint (arXiv:2009.04850).

[22] A. Bhandari, “Unlimited sampling with sparse outliers: Experiments with impulsive and jump or reset noise,” in *IEEE Intl. Conf. on Acoustics, Speech and Sig. Proc. (ICASSP) (to appear)*, 2022.

[23] L. Gan and H. Liu, “High dynamic range sensing using multichannel modulo samplers,” in *IEEE Sensor Array and Multichannel Sig. Proc. Workshop (SAM)*, Jun. 2020.

[24] L. G. Ordoñez, P. Ferrand, M. Duarte, M. Guillaud, and G. Yang, “On full-duplex radios with modulo-ADCs,” *IEEE Open J. of the Comm. Society*, pp. 1279 – 1297, Jun. 2021.

[25] Y. He, C. Liu, J. Qiu, Y. Liu, Y. Li, and J. Wu, “An ENOB-enhanced optical analog-to-digital converter with cascaded step-size MMI and modulo operation,” in *Conference on Lasers and Electro-Optics*. OSA, May 2021.

[26] R. Wiley, H. Schwarzlander, and D. Weiner, “Demodulation procedure for very wide-band FM,” *IEEE Trans. Commun.*, vol. 25, no. 3, pp. 318–327, Mar. 1977.

[27] W. Sun and X. Zhou, “Reconstruction of band-limited signals from local averages,” *IEEE Trans. Inf. Theory*, vol. 48, no. 11, pp. 2955–2963, Nov. 2002.

[28] ——, “Reconstruction of band-limited functions from local averages,” *Constructive Approximation*, vol. 18, no. 2, pp. 205–222, Apr. 2002.

[29] A. Aldroubi, Q. Sun, and W.-S. Tang, “Convolution, average sampling, and a Calderon resolution of the identity for shift-invariant spaces,” *Journal of Fourier Analysis and Applications*, vol. 11, no. 2, pp. 215–244, Feb. 2005.

[30] Z. Song, B. Liu, Y. Pang, C. Hou, and X. Li, “An improved Nyquist–Shannon irregular sampling theorem from local averages,” *IEEE Trans. Inf. Theory*, vol. 58, no. 9, pp. 6093–6100, Sep. 2012.

[31] K. Gröchenig, “Reconstruction algorithms in irregular sampling,” *Mathematics of computation*, vol. 59, no. 199, pp. 181–194, 1992.